Predicting the effect of radiation damage on dark current in a space-qualified high performance CMOS image sensor

Conference or Workshop Item

Jinst

Published by IOP Publishing for Sissa Medialab

Received: *September 27, 2019*
Accepted: *October 16, 2019*
Published: *???, 2019*

21st International Workshop on Radiation Imaging Detectors
7–12 July 2019
Crete, Greece

Predicting the effect of radiation damage on dark current in a space-qualified high performance CMOS image sensor

C. Crews,[a,1] **M.R. Soman,**[a] **D-D. Lofthouse-Smith,**[a] **E.A.H. Allanwood,**[a] **K.D. Stefanov,**[a] **M. Leese,**[a] **P. Turner**[b] **and A.D. Holland**[a]

[a] *Centre for Electronic Imaging, The Open University, Milton Keynes, United Kingdom*
[b] *Teledyne-e2v, Chelmsford, United Kingdom*

E-mail: chiaki.crews@open.ac.uk

Abstract: The CIS115 is a Teledyne-e2v CMOS image sensor with 1504 × 2000 pixels of 7 µm pitch. It has a high optical quantum efficiency owing to a multi-layer anti-reflective coating and its backside illuminated construction, and low dark current due to its pinned photodiode 4T pixel architecture. The sensor operates in rolling shutter mode with a frame rate of up to 7.5 fps (if using the whole array), and has a low readout noise of ~ 5 electrons rms.

The CIS115 has been selected for use within the JANUS instrument, which is a high resolution camera due to launch on board ESA's JUpiter ICy moons Explorer (JUICE) spacecraft in 2022. After an interplanetary transit time of over 7 years, JUICE will spend 3.5 years touring the Jovian system, studying three of the Galilean moons in particular: Ganymede, Callisto and Europa. During this latter part of the mission, the spacecraft and hence the CIS115 sensor will be subjected to the significant levels of trapped radiation surrounding Jupiter.

Gamma and proton irradiation campaigns have therefore been undertaken in order to evaluate both ionising and non-ionising dose effects on the CIS115's dark current performance. Characterisations were carried out at expected mission operating temperatures (−35 ± 10°C) both prior to and post-irradiation. Models of the resulting degradation in dark current behaviour will be combined with expected doses during the JUICE mission in order to predict the performance of the CIS115 at the mission end-of-life.

Keywords: Photon detectors for UV, visible and IR photons (solid-state) (PIN diodes, APDs, Si-PMTs, G-APDs, CCDs, EBCCDs, EMCCDs, CMOS imagers, etc); Radiation damage to detector materials (solid state); Radiation-hard detectors; Space instrumentation

[1] Corresponding author.

https://doi.org/xxxxxxx

Contents

1 Introduction

1.1 JUICE and JANUS

The JUICE (JUpiter ICy moons Explorer) mission is the first L-class mission selected as part of the European Space Agency's (ESA) Cosmic Vision program. It is currently due to launch in 2022, and after a 7.6-year interplanetary cruise the spacecraft will carry out 3.5 years of observations in the Jovian system. In particular, the mission's aim is to characterise conditions that may have led to the emergence of habitable environments on the ocean-bearing icy moons Ganymede, Europa, and Callisto [1]. Its scientific payload consists of 11 instruments, including the high-resolution optical imager JANUS (*Jovis, Amorum ac Natorum Undique Scrutator*). At its core, this camera consists of a greyscale sensor — the CIS115 by Teledyne-e2v — with a filter wheel for selecting various broad and narrow bands in the 340 nm to 1080 nm range [2].

1.2 The CIS115

The CIS115 is a back-illuminated monolithic silicon CMOS active pixel sensor (APS) with 2000 rows $\times$ 1504 columns of 7 µm-pitch pixels, giving an imaging area of 14.0 mm $\times$ 10.5 mm. This is divided into four 376-column blocks, each with a pair (reset and signal) of analogue outputs for correlated double sampling (CDS). Frames are read out in rolling shutter mode, taking $\sim$ 7.5 fps for the full frame (or higher if windowed). The maximum readout rate is 10 Mpixel s^{-1} output^{-1}, but tests described below were carried out at 5 Mpixel s^{-1} output^{-1}, and the sensor will be operated at 2 Mpixel s^{-1} output^{-1} during the JUICE mission [3].

This sensor is manufactured by Tower Jazz in the 0.18 µm process, then back-thinned to ~ 10 µm by Teledyne-e2v. A multi-layer anti-reflection coating is also applied for optimum quantum efficiency performance across a wide optical wavelength range (< 80% between 400–700 nm). Its full well capacity at saturation is 33 ke$^-$ pixel^{-1} and gain 50 µV electron^{-1}. For additional sensor specifications, the reader is referred to table 1 in the CIS115 datasheet [4]; of particular note are its low dark current (20 electrons s^{-1} at 20°C) as well as a low readout noise (5 electrons rms).

The CIS115 has been space-qualified to European Cooperation for Space Standardization (ECSS) guidelines. The radiation qualification was carried out at the Open University in conjunction with testing the effect of the radiation environment on the CIS115 during the JUICE mission. During the qualification, multiple CIS115 devices were exposed to proton and gamma radiation sources in order to explore changes in behaviour with different doses of displacement damage and ionising radiation. Detailed characterisation of the CIS115's dark current behaviour following exposure to each of the radiation sources is presented here.

2 The radiation environment

Before irradiation to the appropriate dose for the JUICE mission, the expected dose at the focal plane was determined using a range of simulation tools. During the interplanetary cruise phase, the JUICE spacecraft will be subjected primarily to energetic solar protons, with the electron flux negligible in comparison. However, it is during the tour of Jupiter and its moons that the trapped electrons and protons within Jupiter's extensive magnetic field will contribute the majority of the overall flux of radiation affecting the spacecraft. These fluxes can be predicted using the Jovian Specification Environment (JOSE) model and the Ganymede Radiation Environment Engineering Tool (GREET) available via the online SPENVIS tool [5].

This radiation will interact with shielding and other components prior to reaching the focal plane array (FPA) where the CIS115 resides. Therefore, a reverse Monte-Carlo analysis of the environmental fluences (from fluxes during each phase multiplied by time spent in each phase — also multiplied by a factor of safety of 2) combined with an up-to-date spacecraft and instrument shielding model was carried out in FASTRAD. The resulting fluences of protons and electrons are plotted in figure 1, illustrating that the trapped electron fluence is expected to be several orders of magnitude higher than the proton fluence. Fluences at each energy are combined with corresponding linear energy transfer (LET) and non-ionising energy loss (NIEL) values to calculate total ionising dose (TID) and displacement damage dose (DDD) respectively.

Thus, the TID for the *total* mission lifetime (i.e. including the interplanetary cruise phase) was predicted to be 44 krad(Si), and the DDD was calculated to be 9.5×10^9 cm^{-2} 10 MeV p$^+$ displacement damage equivalent fluence (DDEF).

3 Radiation campaigns and device characterization

The expected fluences and resulting doses determined above were used to plan gamma and proton radiation campaigns. CIS115 devices were subjected to a range of doses that were chosen such that they covered these expected levels as well as higher doses as an added precaution.

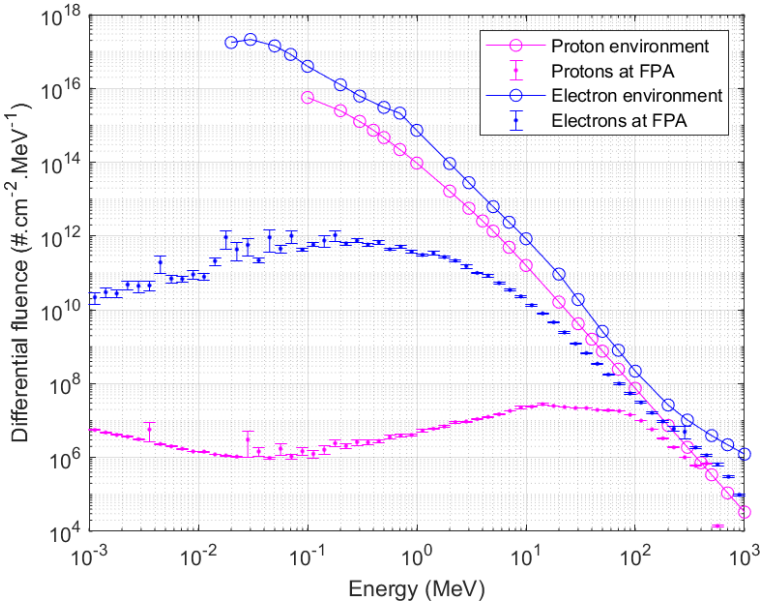

Figure 1. Environmental proton and electron fluences and fluences reaching FPA during 3.5-year tour of Jovian system.

The ESA European Space Research and Technology Centre's (ESTEC) Co-60 facility was used for gamma irradiations; devices were exposed to doses of 50 krad(Si), 100 krad(Si), and 200 krad(Si) whilst biased and at room temperature. Proton irradiations were performed at the Paul Scherrer Institute's Proton Irradiation Facility to doses of 0.5×10^{10}, 1×10^{10}, and 2×10^{10} cm^{-2} 10 MeV p^{+} DDEF, with devices at room temperature and *un*biased in this case.

Dark current characterisations were carried out between −25°C and −50°C both before and after the radiation campaigns. The median of 10 dark frames acquired at each integration time (ranging between 0.1 s and 130 s) were averaged across three repeat runs, and fits to dark signal vs. integration time plots were used to extract the dark current for each pixel.

4 Results and discussion

4.1 Beginning of life

Dark current histograms at the devices' beginning of life (BOL) at −25°C are shown in figure 2a. The mean of the histogram peak values was 0.3 electrons s^{-1} at this temperature. As −25°C is the warmest temperature of the expected operational temperature range of JANUS, this can be taken to be the worst case BOL modal dark current. The analysis of warm-temperature dark current data (+30°C to +40°C) has been reported elsewhere [6].

All devices' BOL dark current histograms displayed a small proportion of higher dark current pixels extending up to approximately 20 electrons s^{-1}. This feature originates mostly from pre-existing defects, but also in part from a "glow" in the corner corresponding to pixel (row 1, col 1) that was seen in all devices (see figure 2b for an example), and which is thought to be a result of hot carrier effects (the generation of optical photons by circuitry outside the image area [7]). One device (15901-17-19) had a greater number of pixels with higher dark currents due to an additional

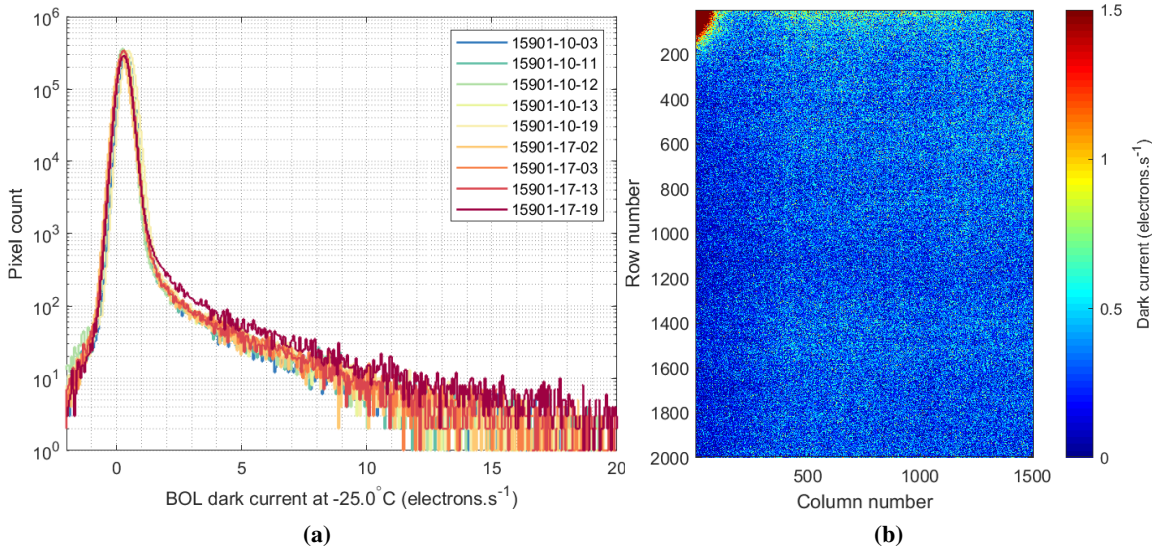

Figure 2. (a) BOL dark current histograms for all devices used; (b) DC map for device 15901-17-13 at −25°C.

bright region centred on pixel (row 1, col 376) at the corner of column block 1, which would have declassified the device from being suitable for flight. These effects were not significant compared to the DDD-induced dark current levels discussed below, particularly at the short integration times expected to be used on JANUS.

4.2 Post-gamma irradiation

The change in dark current (ΔDC) at −27.5°C in devices irradiated to 50 krad(Si), 100 krad(Si), and 200 krad(Si) dose levels are presented in figure 3. In general, these displayed Gaussian distributions as expected from the creation of electron-hole pairs (that generate defects if they escape recombination) uniformly across all pixels.

The 50 krad(Si) dose level had a minimal effect on dark current, with the ΔDC histogram peak centred at 0.20 electrons s^{-1}. After a 100 krad(Si) dose, there was a greater shift in the ΔDC peak centre to 0.54 electrons s^{-1}. In addition, a tail-like feature appeared that mostly originated from the combination of pixels from two regions: one at the corner where the "glow" was seen at BOL, plus a new region post-irradiation centred at (row 1000, col 1) that may be from added hot carrier effects from peripheral circuitry affected by the ionising radiation (see figure 4). Once again, these are not expected have much impact on scientific observations at the short integration times and exposure levels expected for JANUS — from figure 3b, it can be seen that there are very few pixels affected. Lastly, the 200 krad(Si) histogram showed an even greater peak shift to a ΔDC of 2.8 electron s^{-1}; the minor peak centred at zero is a result of defective pixels along two rows, and no additional "glow" regions were observed.

Gaussian fits to these peaks (as shown in figure 3(b)) were used to extract their means (μ) and standard deviations (σ), which were then plotted against TID. Fits made to these data resulted in equations that could be used to find μ and σ at a particular TID, at −27.5°C — the highest

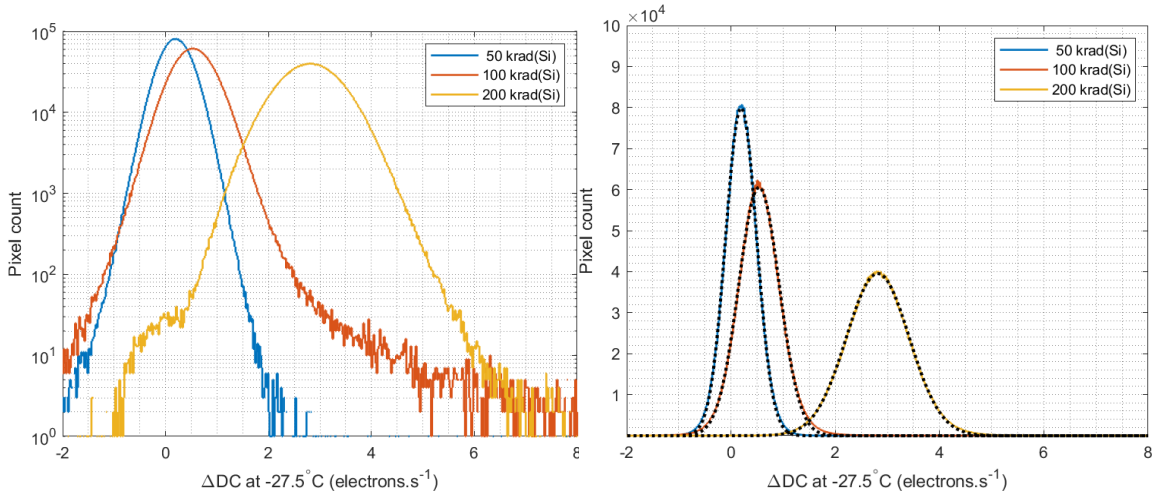

Figure 3. ΔDC histograms (bin width 0.02 electrons s^{-1}) post-gamma irradiation (a) with logarithmic y-axis, and (b) with linear y-axis and including Gaussian fits (black dashed lines).

temperature i.e. worst case out of the data available. Hence, these could be used to predict the Gaussian distribution of pixel ΔDCs by using the Gaussian probability density equation.

4.3 Post-proton irradiation

ΔDC histograms post-proton irradiation for different proton doses at −25°C and −35°C are shown in figure 5 for comparison. These histograms had peak ΔDC populations centred close to zero electrons s^{-1} for all devices and doses. There is a general trend of a slight increase in this modal ΔDC with increasing radiation level that is attributed to the low level of TID incurred during the proton irradiations.

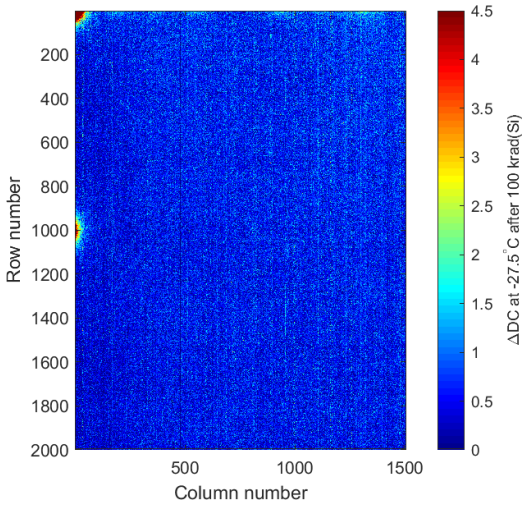

Figure 4. ΔDC map for device irradiated to 100 krad(Si).

More significantly, high ΔDC pixel tails resulting from DDD-induced defects are seen in all irradiated devices' histograms. These displacement defects are formed only in certain pixels as protons travel through the silicon lattice, and the affected pixels are randomly spatially distributed across each device. Note that the tails are noticeably reduced in their extent at the lower temperature regime of figure 5b. Overall, this degradation was less significant than originally expected, and led to the revision of the mission operating temperature from −50 ± 5°C to −35 ± 10°C.

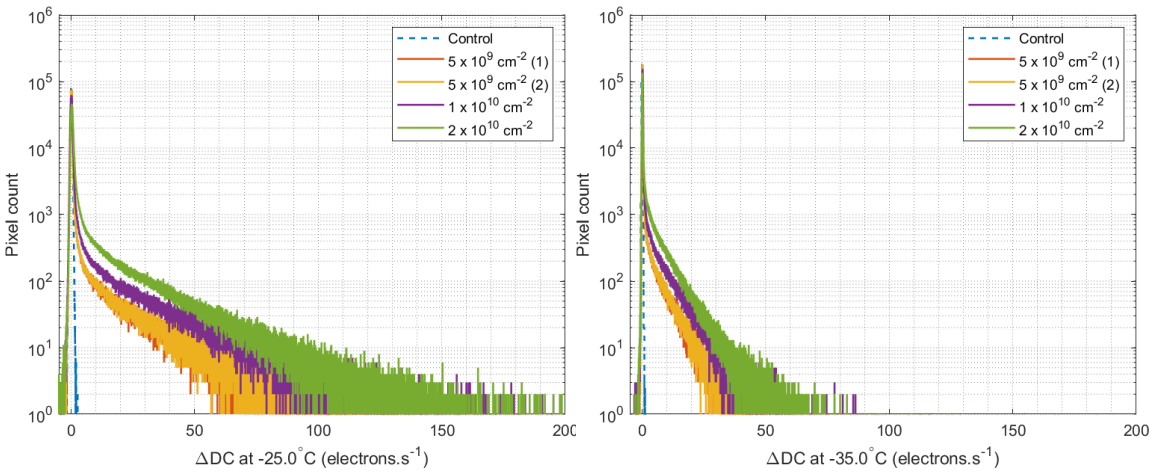

(a) **(b)**

Figure 5. ΔDC histograms (bin width 0.02 electrons s^{-1}) post-proton irradiation (a) at −25°C, and (b) at −35°C.

These high ΔDC, or "hot pixel", tails have previously been modelled as an exponential distribution after normalising counts at each ΔDC [8]. The histograms were thus dose-normalised and combined for each temperature, and fit to the following equation:

$$f(x) = a \cdot e^{-a(x-b)} \tag{4.1}$$

An example of this is plotted in figure 6a. Values of $-b$ (location parameter) and $1/a$ (scale parameter) were then plotted against temperature (figure 6b), and exponential fits were made such that for a known DDD and operating temperature, it was possible to work back to the expected tail shape.

4.4 Predicted end-of-life distribution

Using the fits described in section 4.2, the predicted Gaussian ΔDC histogram for the JUICE mission EOL TID at −27.5°C had μ and σ of 0.15 electrons s^{-1} and 0.30 electrons s^{-1} respectively. This distribution was used to create a cumulative distribution function (CDF), and the inverse of this was sampled using 1502 × 2000 randomly generated values (the inverse transform sampling method [9]) to assign predicted TID-induced ΔDC values to each pixel. The DDD-induced exponential tail distribution at −27.5°C was also calculated and scaled by the expected EOL DDD level. The number of pixels affected by DDD defects in this scenario was extracted, and this number of samples were taken from the distribution using the same method.

The randomly sampled values from both the TID-induced Gaussian and the DDD-induced exponential distributions were then combined — where pixels with no DDD-induced defects were

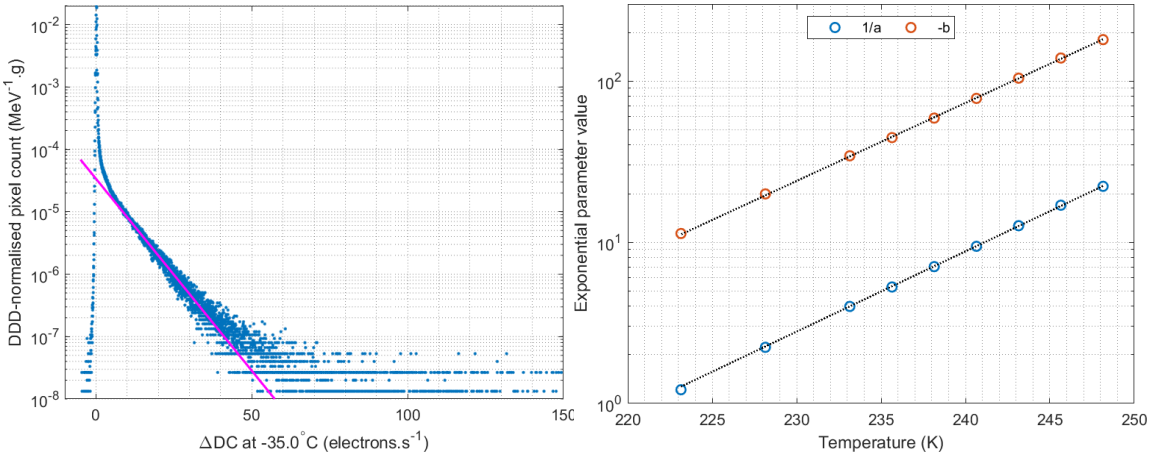

(a) **(b)**

Figure 6. (a) Sample exponential fit to "hot pixel" tails in dose-normalised ΔDC histograms; (b) change in ΔDC tail fits' exponential parameters with temperature.

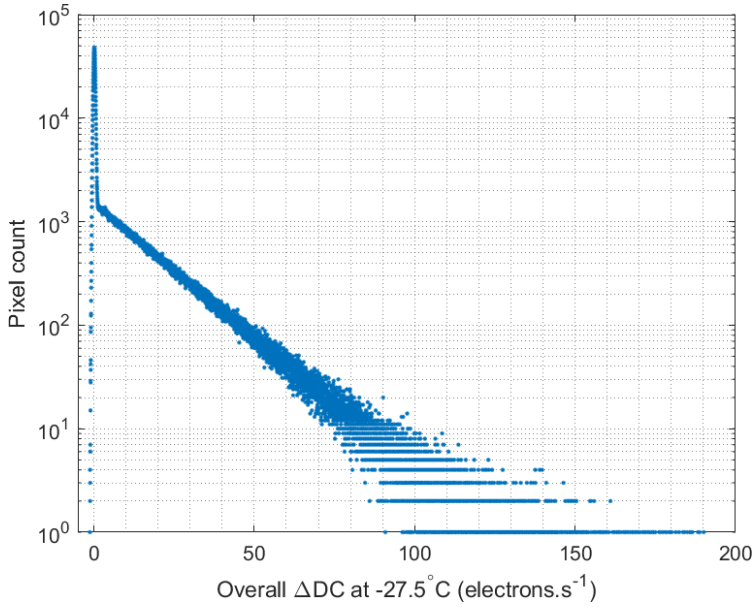

Figure 7. Combined predicted TID and DDD-induced ΔDC distribution for the CIS115 on JANUS at the JUICE mission EOL (including a ×2 factor of safety).

assigned a value of zero ΔDC prior to summation — resulting in the distribution shown in figure 7 for the overall EOL ΔDC.

5 Summary and outlook

The predicted ionising and non-ionising radiation dose that the JANUS camera on JUICE is expected to be subjected to mostly originates from trapped electrons in the Jovian environment. Both TID and DDD effects on dark current were therefore tested using gamma and proton irradiations respectively.

For the former, the key change observed was the shift of modal ΔDC to higher values with increasing dose — these could be modelled by Gaussian fits to the peaks. For the proton irradiations, the important result was the large increase in dark currents in some pixels, creating a hot pixel tail in the ΔDC histograms, whilst the majority of pixels were largely unaffected. The extent of the tail, i.e. the maximum ΔDC relative to BOL dark currents, could be reduced by lowering the operating temperature. The magnitudes of the tails were linear with DDD and could be modelled with an exponential fit.

Overall, in the JUICE radiation environment and under JANUS operating conditions, the CIS115's dark current performance is expected to be dominated by the hot pixel tail generated by displacement damage, since the additional contribution from the small increase in average pixel dark current is negligible with respect to the device's readout noise of 5 e^- rms.

Acknowledgments

The authors would like to acknowledge Vincenzo della Corte (IAPS-INAF) for providing the particle fluence data from FASTRAD simulations. The Open University role on the JANUS consortium is funded by the U.K. Space Agency.

References

[1] JUICE Science Working Team, *JUpiter ICy Moons Explorer - Exploring the Emergence of Habitable Worlds around Gas Giants*, Definition Study Report ESA/SRE(2014)1 (2014).

[2] D. Greggio, M. Munari, D. Magrin, R. Paolinetti, M. Barilli, V. Della Corte et al., *Modeling the JANUS stray-light behavior*, *Proc. SPIE* **10698** (2018) 106984V.

[3] V. Della Corte et al., *Scientific objectives of JANUS Instrument onboard JUICE mission and key technical solutions for its Optical Head*, in *Proceedings of the IEEE International Workshop on Metrology for AeroSpace*, Torino, Italy, 19–21 June 2019, pp. 324–329.

[4] e2v technologies, *CIS115 Back-Side Illuminated (BSI) CMOS Image Sensor Datasheet (A1A-785580 V1)*, (2016).

[5] European Space Agency, *SPENVIS (The Space Environment Information System)*, https://www.spenvis.oma.be (2018).

[6] D.D. Lofthouse-Smith, M.R. Soman, E.A.H. Allanwood, K.D. Stefanov, A.D. Holland, M. Leese et al., *Thermal annealing response following irradiation of a CMOS imager for the JUICE JANUS instrument*, 2018 *JINST* **13** C03036.

[7] T. Greig, A. Holland, D. Burt and A. Pike, *CMOS pixel structures optimised for scientific imaging applications*, *Proc. SPIE* **6660** (2007) 66600T.

[8] C. Virmontois, V. Goiffon, P. Magnan, S. Girard, O. Saint-Pe, S. Petit et al., *Similarities between proton and neutron induced dark current distribution in CMOS image sensors*, *IEEE Trans. Nucl. Sci.* **59** (2012) 927.

[9] B.A. Stickler and E. Schachinger, *Random Sampling Methods*, in *Basic Concepts in Computational Physics*, 2nd edition, Springer (2016).